



Endoscopic Hemostasis in Porcine Gastrointestinal Tract Using CO₂ Low-Temperature Plasma Jet

Kurosawa, Manabu ; Takamatsu, Toshihiro ; Kawano, Hiroaki ; Hayashi, Yuta ; Miyahara, Hidekazu ; Ota, Syosaku ; Okino, Akitoshi ; Yoshida, ...

(Citation)

Journal of Surgical Research, 234:334-342

(Issue Date)

2019-02

(Resource Type)

journal article

(Version)

Accepted Manuscript

(Rights)

© 2019 Elsevier.

This manuscript version is made available under the CC-BY-NC-ND 4.0 license
<http://creativecommons.org/licenses/by-nc-nd/4.0/>

(URL)

<https://hdl.handle.net/20.500.14094/90006430>



Revised
2018/08/03

Endoscopic Hemostasis in Porcine Gastrointestinal Tract using CO₂ Low Temperature Plasma Jet

Manabu Kurosawa, MD,^a Toshihiro Takamatsu PhD,^{b,c,*} Hiroaki Kawano, PhD,^d Yuta Hayashi,^d Hidekazu Miyahara, PhD,^d Syosaku Ota, PhD,^e Akitoshi Okino, PhD,^d Masaru Yoshida, MD, PhD,^{a,f,g}

^aDivision of Gastroenterology, Department of Internal Medicine, Kobe University Graduate School of Medicine, Kobe, Hyogo, Japan

^b Research Institute for Biomedical Sciences, Tokyo University of Science, Noda, Chiba, Japan

^c Exploratory Oncology Research & Clinical Trial Center, National Cancer Center Hospital East, Kashiwa, Chiba, Japan

^dInstitute of Innovative Research, Tokyo Institute of Technology, Yokohama, Kanagawa, Japan.

^eDepartment of Product and Interior Design, Kobe Design University, Kobe, Hyogo, Japan.

^fDivision of Gastroenterology, Department of Internal Medicine, Kobe University Graduate School of Medicine, Kobe, Hyogo, Japan; Division of Metabolomics Research, Department of Internal Related, Kobe University Graduate School of Medicine, Kobe, Hyogo, Japan; AMED-CREST.

^gAMED, Kobe, Hyogo, Japan.

*Corresponding author:

Toshihiro Takamatsu, PhD.

Research Institute for Biomedical Sciences

Tokyo University of Science

2669 Yamazaki, Noda, Chiba, Japan

E-mail : takamatsu@rs.tus.ac.jp

Author contributions:

MK, TT and MY designed and conducted the experiment.

HK, YH, HM, SO and AO developed and setup the plasma device.

ABSTRACT

Background: Recently, atmospheric Low Temperature Plasma(LTP) has attracted attention as a novel medical tool that might be useful for achieving hemostasis. However, conventional plasma sources are too big for use with endoscopes, and the efficacy of LTP for achieving hemostasis in cases of gastrointestinal bleeding is difficult to investigate. In this study, to solve the problem, we developed a 3D printed LTP jet which has a diameter of 2.8 mm and metal body for endoscopic use. And the characteristics, hemostasis efficacy and safety were investigated.

Materials and Methods: As investigation of the basic characteristics of the developed plasma jet, the electron densities, gas temperatures, and reactive species were measured by emission spectroscopy and thermocouple. To evaluate the efficacy of such hemostatic treatment, porcine gastrointestinal bleeding was treated with the device. In addition, to investigate the safety of such treatment, the CO₂ LTP-treated tissue was compared with tissue that was treated with clipping- or argon plasma coagulation (APC)-based hemostasis for 5 days, and hematoxylin and eosin staining was used to evaluate tissue damage in the treated regions.

Results: The measurement of emission spectroscopy, the power, and the electron density of various gas plasmas suggested that a high density (10^{14} cm^{-3}) LTP of CO₂ was generated by the LTP jet and the gas temperature was 41.5°C at 3 mm from the outlet of LTP. And the CO₂ LTP achieved hemostasis of oozing blood with 70±20 s. In addition, the CO₂ LTP gave earlier recovery than clipping- or APC-based hemostasis, and the treated regions had no damage by the CO₂ LTP treatment.

Conclusions: These results indicated that the developed LTP plasma jet has potential to be used for endoscopic hemostasis.

1. Introduction

Gastrointestinal bleeding is often fatal, and it can also occur as a complication of endoscopic interventions, such as endoscopic mucosal resection or endoscopic submucosal dissection. There are many kinds of endoscopic treatment for gastrointestinal bleeding, e.g., hemostatic clipping, ethanol injections, high-frequency radiowave coagulation, argon plasma coagulation (APC), and thrombin injections. However, there are problems with each of these hemostatic methods [1-3]. For example, hemostatic clipping requires a high level of skill, and clip placement can sometimes restrict other procedures. In addition, ethanol can cause severe ulcers around the treated area, and thermal coagulation, such as high-frequency radiowave coagulation and APC, can damage the treated area and carry a risk of perforation. Thrombin-based hemostasis is safe and easy, but its efficacy is insufficient to allow it to be used as a first treatment. Therefore, it is necessary to develop a safer, more effective, and easy-to-use hemostatic method.

Recently, low temperature plasma (LTP) has attracted attention as a novel medical tool, and its efficacy at achieving bacterial inactivation [4-7], wound healing [8, 9], and blood coagulation [10-12] has been investigated. The mechanism by which LTP induces blood coagulation is considered to involve reactions between reactive oxygen species (ROS) and blood coagulation factors [10], and a number of studies have investigated LTP-based blood coagulation in vivo and in vitro [13-18]. According to these studies, LTP promotes the blood coagulation cascade or aggregates proteins by OH radicals and other reactive species. LTP activates multiple factors in the intrinsic and extrinsic cascade of blood coagulation, and fibrin is produced by blood coagulation. These fibrin or aggregated proteins close the broken blood vessels to achieve hemostasis [11, 13, 18]. On the other hand, the clipping compresses and closes the broken blood vessels physically to achieve hemostasis [19]. Heat coagulation such as APC achieves hemostasis by closing the broken vessels with heat degeneration of the broken blood vessels and surrounding proteins [20]. In addition, in these studies, bleeding was induced by surgically wounding organs or the gastrointestinal tract from outside the body with an open surgical method. Although there have been a few studies of LTP devices that can be used through an endoscope, no previous studies have examined the use of LTP to induce hemostasis in the gastrointestinal tract through an endoscope [21]. This is because conventional manufacturing methods limit the size of endoscopic LTP devices. In addition, since most of the previously reported LTP devices were only able to produce LTP from argon (Ar) or helium (He), it would be difficult to use them to produce ROS and reactive nitrogen species stably in the gastrointestinal tract, which is an enclosed space. Takamatsu et al. established a method for producing a smaller LTP source that can use various gases [22], and they succeeded in miniaturizing the tip of the plasma source (diameter: 3.7 mm) by using a 3D printer [23]. This new device can produce plasma not only from Ar and He, but also from oxygen (O₂), carbon dioxide (CO₂), and

nitrogen (N₂). CO₂ exhibits good bioabsorbability, and the achievement of hemostasis with CO₂-based LTP (hereafter referred to as CO₂ LTP) during open surgery has already been reported [16]. It would be useful if CO₂ LTP could also be used to achieve hemostasis in the gastrointestinal tract under endoscopy, as it would be less invasive and exhibit high bioabsorbability. In this study, to adapt LTP for use during the hemostatic treatment of gastrointestinal bleeding, we evaluated the efficacy and safety of CO₂ LTP-based hemostatic treatment using a 3D printed LTP jet for porcine gastrointestinal bleeding.

2. Materials and methods

2.1. Low temperature plasma jet

The plasma source was designed with a diameter of 2.8 mm via 3D-CAD because the diameter of the forceps port of an upper gastrointestinal endoscope is 3.2 mm. The structure of the plasma jet is shown in Fig1. (a). This plasma jet is composed of an internal electrode to which a high voltage is applied, a gas supply unit, an insulating unit, and a main frame with a plasma outlet port. The main frame and internal electrode were made from titanium Ti64 using a 3D metal printer (M280, Electro Optical Systems Inc.). This 3D printer makes a product from material powder by laser-sintering[24, 25]. An alumina tube with an inside diameter of 1.5 mm, outside diameter of 2.5 mm, and length of 8 mm was used for the insulating section. The distance between the tip of the internal electrode and the outlet port was an inter-electrode distance of 0.5 mm.

Upon applying a high voltage between the grounded main frame and the internal electrode, a discharge is caused between the electrodes at the tip and plasma is generated. The gas flow blows the plasma out from the 1 mm-diameter outlet port. As a consequence, the target is irradiated with plasma afterglow (also referred to as plasma flare), which includes excited atoms/molecules, ions, electrons, and reactive species without current flows. Therefore, it is possible to irradiate with the plasma without producing damage due to discharge. The afterglow length changes with the plasma gas species because of the lifetimes of the excited states of the relevant atoms or molecules.

Fig. 1(b) shows an overview of the plasma source, including each assembled part. Because a 2 m length was required to support insertion into the endoscope, the total length of wiring and the gas inlet tube was 2 m. The high voltage and ground side wires were installed inside and outside the gas tube, respectively. Fig. 1 (c) shows an image of device insertion into the forceps port of the endoscope. Gas and electric power were supplied from the termination and connected terminals, respectively. This study used a high-voltage power supply (DFMJ 01, Plasma Concept Tokyo) modified to 2.25 kV and 50 Hz and a gas flow rate of 1 L/min.

2.2. Measurement of spectroscopy

To determine the fundamental characteristics of the plasma source, the emissions from excited

atoms and molecules were measured using a spectroscope [Maya2000 Pro (200–1100 nm), Ocean Optics, Inc.] and a 50-cm focal length Czerny–Turner monochromator (wavelength resolution: 0.027 nm) equipped with a photo multiplier (R928, Hamamatsu Photonics Company, Hamamatsu, Japan). The plasma emission was measured at a distance of 3 mm, with a 1 mm quartz glass plate sandwiched between an optical fiber and the plasma source outlet. The fiber faced the plasma source outlet from the axial direction [22, 26, 27]. The purpose of the quartz glass tube was to protect the optical fiber so that it was not directly exposed to the plasma. The electron density, which is among the most important plasma parameters, was calculated from the spread of the emission spectrum of the H β line (486.13 nm) [28, 29].

2.3. Plasma gas temperature measurement

The plasma temperature was measured using a thermocouple. The plasma source and thermocouple were placed perpendicular to each other, 3 mm from the plasma outlet. For the measurement, a K-type thermocouple with a diameter of 1 mm and length of 50 mm was used with argon, helium, oxygen, nitrogen, air, and carbon dioxide as the working gases.

2.4. Investigation of plasma-induced hemostasis and its safety in the porcine stomach

Two living adult LDW pigs, which heart rate, blood pressure and PT-INR were about 100 bpm, 100/40 mmHg and 1.2, was used in this study. Ketamine (10 mg/kg), xylazine (2 mg/kg), and atropine sulfate (0.5 mg/head) were used as premedication and were intramuscularly injected. Isoflurane (5%) was used to induce anesthesia. After tracheal intubation, anesthesia was maintained with 2-3% isoflurane. Peripheral intravenous access was maintained using a 60 ml/h drip infusion of lactate Ringer's solution through an auricular vein. Under general anesthesia, an endoscope (EG-580RD, Fujifilm Co., Japan) was inserted into the pig's stomach. The plasma source made with the 3D printer was delivered through the endoscope. All of the procedures and protocols were approved by the animal care and use committee of IVTeC Japan (IVT15-05).

In this study, bleeding wounds were created with biopsy forceps (Radial Jaw 4, Olympus, Japan). As shown Fig. 2(b) – (d), several biopsies could cause mucosal damage. The size of wound was 5.3 ± 2.5 mm², and the state of bleeding was oozing. The plasma source was placed near to the targeted bleeding wound, and CO₂ LTP was used to irradiate it until hemostasis was achieved. All data were obtained from three replicate experiments in each pig (N=6). The tip of the plasma source was kept at a distance of 1-2 mm from the bleeding source and did not come into direct contact with the mucosa. Hemostasis was also achieved using APC and clipping. Each wound site was subjected to endoscopic follow-up examinations at 1, 3, and 5 days after treatment. On the last day of the study, the pig was euthanized by incising the aorta under general anesthesia. To evaluate the mucosal damage and

hemostasis at each treatment site, the gastric mucosa was harvested immediately after treatment and 5 days after treatment and examined for tissue changes using optical microscopy and hematoxylin and eosin (H&E) staining.

3. Results and Discussion

3.1. Plasma emission spectra and characteristics

We generated plasmas from various gases: helium, argon, air, oxygen, nitrogen, and carbon dioxide. Fig. 3 shows photographs of the plasmas generated from each gas. An afterglow plasma approximately 3 mm in size can be confirmed visually. Furthermore, plasmas are generated stably with the plasma jet inserted within the forceps port. Fig. 4 shows the corresponding emission spectra. The emission spectra of the molecular, atomic, and ion lines caused from the working gases were observed. Table 1 shows the electron densities (n_e), the power (P) and plasma gas temperatures (T_g) of each gas species. The electron densities of the helium and argon plasmas are $2.8 \times 10^{14} \text{ cm}^{-3}$ and $5.9 \times 10^{14} \text{ cm}^{-3}$, respectively. In the plasma jet, the electron density of the plasma was of the order of 10^{14} cm^{-3} . Based on previous research [26, 30, 31], our plasma jet generates high-level density plasma in LTP device. Since H_β line was overlap by molecular line in the emission of plasma using molecular gas as a process gas, electron density was observed only in Ar and He. The powers are 0.6, 0.8, 1.3, 1.8 2.8, and 3.1 W, for helium, argon, air, carbon dioxide, nitrogen, and oxygen, respectively. Oshita et al. reported that the rate of variation of the OH rotational temperature was almost the same as that of the plasma gas temperature as measured using a thermocouple [27]. Therefore, in this study, the plasma gas temperature was measured with thermocouple. The plasma temperatures are 37, 39, 41, 50, 53, and 73°C, for argon, carbon dioxide, oxygen, nitrogen, air, and helium, respectively. The plasma temperatures of argon, carbon dioxide, and oxygen are close to or less than that of a living body.

3.2. Efficacy of LTP-based hemostasis in the porcine stomach

The bleeding wounds made with endoscopic biopsy forceps are shown in Figs. 5 (a-1), (b-1), and (c-1). Figure 5(a-2) shows that the bleeding wound in Fig. 5(a-1) was treated with clips. The bleeding vessel was compressed with clips, and hemostasis was achieved. Figure 5(a-3) shows the treated site at 1 day after treatment. One clip had dropped off. There was no pressure around the bleeding vessel, and hemostasis had been maintained by vessel remodeling involving platelets and fibrin. Figure 5(a-4) shows the treated site at 3 days after treatment. It had been covered by the regenerating epithelium. As is shown in Fig. 5(a-5), few changes were seen between 3 and 5 days after treatment, and small clip scars were noted.

The bleeding wound shown in Fig. 5(b-1) was coagulated with APC, as shown in Fig. 5(b-2). The bleeding wound and surrounding tissue were damaged and carbonized. As is shown in Fig. 5(b-3), at 1 day after treatment the carbonized tissue had disappeared, heat-damaged white mucosal tissue was noted, and a shallow region of tissue erosion was seen in part of the treated site. At 3 days after the APC treatment, the heat-damaged white mucosal tissue had also disappeared, and only the shallow region of tissue erosion was observed, as shown in Fig. 5(b-4). After 5 days, the regenerating epithelium had started to cover the erosion defect, as is shown in Fig. 5(b-5). The wound treated with APC had the largest mucosal defect (in terms of area) of all of the treated wounds at 5 days after treatment.

The bleeding wound shown in Fig. 5(c-1) was treated with CO₂ LTP through an endoscope. During the irradiation of CO₂ LTP, no change was observed in pig's vital signs. The bleeding was gradually coagulated from where the CO₂ LTP was irradiated, although the wound kept bleeding when CO₂ gas alone was irradiated. After 70±20 s plasma treatment, the bleeding had coagulated sufficiently. After treatment, the coagulated site was washed with water several times, but no re-bleeding occurred, as shown in Fig. 5(c-2). In addition, there were no visible changes around the LTP-treated mucosa. These results suggest that the coagulation mechanism of LTP does not involve angiopressure or heat. Instead, the CO₂ LTP treatment caused blood coagulation at low temperature, and the resultant small clots sealed the broken vessels. Therefore, there is a possibility that fibrinogen and platelet aggregation are promoted by LTP treatment. As a result, LTP rapidly closes the broken blood vessels with small clots and it achieves hemostasis earlier than the natural course.

The next day, there was no damage around the LTP-treated mucosa, as shown in Fig. 5(c-3). At 3 days after the plasma treatment, the treated site had started to be covered by the regenerating epithelium Fig. 5(c-4). In addition, at 5 days after the treatment the wound had become less red, as shown in Fig. 5(c-5). In comparison with the defect left after the APC treatment, the mucosal defect observed after the CO₂ LTP treatment was smaller and had healed faster.

3.3. Microscopic examinations of gastric tissue

As follow-up evaluation of each treatment, we prepared specimens of normal gastric mucosa (Fig. 6), gastric mucosa immediately after each treatment (Fig. 7) and gastric mucosa 5 days after each treatment (Fig. 8), and observed them by using optical microscopy and H&E staining.

Figures 6(a) and (a') show the intact porcine gastric mucosa. The mucosal epithelium, submucosal layer, and muscle layer could be observed. Figures 7 and 8 show H&E-stained histological sections immediately and 5 days after clipping, APC, or CO₂ LTP treatment. In Figs. 7(a) and (a'), the bleeding site had been covered by the surrounding mucosa, which was closed with clips. After 5 days, inflammatory cells had appeared around the treated site, and the mucosal epithelium had partially regenerated (Figs. 8(a) and (a')). In Figs. 7(b) and (b'), which shows an APC-treated wound, heat damage

can be seen from the mucosal epithelium to the muscular layer of the mucosa, and broken red blood cells were found on the surface of the mucosa. After 5 days, more inflammatory cells were observed around the treated area, and slight regeneration of the mucosal epithelium was noted (Figs. 8(b) and (b')). In Figs. 7(c) and (c'), which shows a wound that was treated with CO₂ LTP treatment, no damage was observed under the mucosal epithelium, and the red blood cells on the mucosal surface remained intact. Fibrous membrane like structure was seen on the surface layer immediately after LTP treatment. After 5 days, the appearance of inflammatory cells in tissues of LTP treatment was slighter than that of APC. And regeneration of the mucosal epithelium was seen (Figs. 8(c) and (c')).

The physiological mechanism responsible for hemostasis is based on the balance between coagulation and anticoagulation. Coagulation mainly involves fibrinogenesis and platelet adhesion and aggregation. It does not usually inhibit blood flow in blood vessels, but once bleeding from blood vessels occurs, it acts to block blood flow in the broken vessels by inducing blood clots. After hemostasis has been achieved, the broken vessels are repaired, and reperfusion starts. The mechanism by which hemostasis is induced involves blood cells, serous proteins, and blood vessel wall components. These elements induce hemostasis; i.e., a state in which extravasation from broken vessels has stopped, via complex interactions. In this experiment, we confirmed that hemostasis can be achieved with CO₂ LTP treatment and considered the mechanisms by which hemostasis was induced by CO₂ LTP treatment, hemostatic clipping, and APC. Hemostatic clipping sealed the broken vessels by applying physical pressure to them from outside, as shown in Fig. 7(a). APC sealed the broken vessels and surrounding tissue by degenerating proteins thermally, as shown in Fig. 7(b). However, the CO₂ LTP treatment induced hemostasis via a different mechanism to these two techniques, as shown in Fig. 7(c). It is suggested that platelet adhesion, fibrinogenesis, or protein aggregation, which are promoted by CO₂ LTP treatment, sealed the broken vessels, leading to hemostasis [10, 11, 17, 18]. In addition, little thermal damage was seen around the bleeding wound treated with CO₂ LTP. Therefore, this suggests that little damage was caused to the mucosal epithelium, and so the wound healed faster.

From above result, we consider LTP is less invasive and might be useful for hemostasis against fragile tissue which we cannot treat with other devices. For example, gastrointestinal bleeding in patients taking antithrombotic agents is sometimes difficult to achieve complete hemostasis with a single hemostatic device and hemostasis is performed with an appropriate device according to each case. They often repeat bleeding even after hemostasis treatment, and repeated treatments accumulate damage to the tissue and increase the risk of perforation. For these reasons, there is a need for a hemostasis method of new mechanism or a safer hemostasis method with less tissue damage, and in that sense LTP may be useful. In addition, Nomura et al. reported that blood mixed with anticoagulant drug was coagulated by LTP in their experiment, so we consider there is a possibility that LTP can be used also for hemostasis against gastrointestinal bleeding of patients taking anticoagulant drugs. To use the LTP in practical use, although more rapid hemostasis is

required, there are much rooms for improvements such as adjusting conditions (e.g. the gas temperature, electric power and gas flow rate) or combination use of a substance that promotes blood coagulation. Therefore, the developed LTP plasma jet could be a promising tool for endoscopic hemostasis.

4. Conclusion

In this study, we made a 3D printed LTP jet for use with an endoscope, and investigated the parameters of plasma generated by the jet. We also used it to perform hemostatic treatment against porcine gastrointestinal bleeding. In addition, the efficacy and safety of CO₂ LTP treatment were evaluated. As a result, plasma emission of carbon dioxide was observed, and atomization of CO₂ plasma was confirmed. The power was 1.8 W, and gas temperature was 41.5 °C. It was confirmed that CO₂ LTP treatment achieved hemostasis within 70±20 s, and that it caused little thermal damage around the treated mucosa. These findings suggest that CO₂ LTP mainly induces hemostasis through blood coagulation and protein aggregation. Therefore, in comparison with clipping or APC, CO₂ LTP could be easier to perform and less invasive. Furthermore, the LTP-treated mucosa healed faster than those treated using the other techniques. To use LTP in practical treatment, further improvement of the hemostasis effect of LTP is required, and we are planning to solve this issue in future study.

Acknowledgment

This study was supported by the Research Center for Biomedical Engineering, Grant-in-Aid for Young Scientists ((B) Grant Number 16K17536) and the Program for Creating Start-ups from Advanced Research and Technology (Grant Number 924083). This article was proofread by Medical English Service. The authors thank Plasma Concept Tokyo, Inc., for their support and collaboration.

References

- [1] Gralnek IM, Barkun AN, Bardou M Management of Acute Bleeding from a Peptic Ulcer. *New England Journal of Medicine* 2008;359:928-937.
- [2] Cipolletta L, Bianco MA, Rotondano G, Piscopo R, Prisco A, et al. Prospective comparison of argon plasma coagulator and heater probe in the endoscopic treatment of major peptic ulcer bleeding. *Gastrointestinal Endoscopy* 1998;48:191-195.
- [3] Cipolletta L, Bianco MA, Marmo R, Rotondano G, Piscopo R, et al. Endoclips versus heater probe in preventing early recurrent bleeding from peptic ulcer: A prospective and randomized trial. *Gastrointestinal Endoscopy* 2001;53:147-151.
- [4] Takamatsu T, Kawate A, Uehara K, Oshita T, Miyahara H, et al. Bacterial inactivation in liquids using multi-gas plasmas. *Plasma Medicine* 2012;2.

- [5] Pei X, Lu X, Liu J, Liu D, Yang Y, et al. Inactivation of a 25.5 μ m *Enterococcus faecalis* biofilm by a room-temperature, battery-operated, handheld air plasma jet. *J Phys D Appl Phys* 2012:45.
- [6] Takamatsu T, Uehara K, Sasaki Y, Hidekazu M, Matsumura Y, et al. Microbial Inactivation in the Liquid Phase Induced by Multigas Plasma Jet. *PLoS ONE* 2015;10:e0132381.
- [7] Takamatsu T, Kawano H, Sasaki Y, Uehara K, Miyahara H, et al. Imaging of the *Staphylococcus aureus* Inactivation Process Induced by a Multigas Plasma Jet. *Current Microbiology* 2016;73:766-772.
- [8] Heinlin J, Morfill G, Landthaler M, Stolz W, Isbary G, et al. Plasma medicine: possible applications in dermatology. *JDDG: Journal der Deutschen Dermatologischen Gesellschaft* 2010;8:968-976.
- [9] Isbary G, Morfill G, Schmidt HU, Georgi M, Ramrath K, et al. A first prospective randomized controlled trial to decrease bacterial load using cold atmospheric argon plasma on chronic wounds in patients. *British Journal of Dermatology* 2010;163:78-82.
- [10] Kalghatgi SU, Fridman G, Cooper M, Nagaraj G, Peddinghaus M, et al. Mechanism of Blood Coagulation by Nonthermal Atmospheric Pressure Dielectric Barrier Discharge Plasma. *IEEE Transactions on Plasma Science* 2007;35:1559-1566.
- [11] Ikehara S, Sakakita H, Ishikawa K, Akimoto Y, Yamaguchi T, et al. Plasma Blood Coagulation Without Involving the Activation of Platelets and Coagulation Factors. *Plasma Processes and Polymers* 2015;12:1348-1353.
- [12] Ke Z, Huang Q Haem-assisted dityrosine-cross-linking of fibrinogen under non-thermal plasma exposure: one important mechanism of facilitated blood coagulation. *Scientific Reports* 2016;6:26982.
- [13] Fridman G, Peddinghaus M, Balasubramanian M, Ayan H, Fridman A, et al. Blood Coagulation and Living Tissue Sterilization by Floating-Electrode Dielectric Barrier Discharge in Air. *Plasma Chemistry and Plasma Processing* 2006;26:425-442.
- [14] Hoffmann M, Ulrich A, Habermann JK, Bouchard R, Laubert T, et al. Cold-Plasma Coagulation on the Surface of the Small Bowel Is Safe in Pigs. *Surg Innov* 2016;23:7-13.
- [15] Aleinik A, Baikov A, Dambaev G, Semichev E, Bushlanov P Liver Hemostasis by Using Cold Plasma. *Surgical Innovation* 2017:1553350617691710.
- [16] Nomura Y, Takamatsu T, Kawano H, Miyahara H, Okino A, et al. Investigation of blood coagulation effect of nonthermal multigas plasma jet *in vitro* and *in vivo*. *Journal of Surgical Research* 2017;219:302-309.
- [17] Ikehara Y, Sakakita H, Shimizu N, Ikehara S, Nakanishi H Formation of Membrane-like Structures in Clotted Blood by Mild Plasma Treatment during Hemostasis.

Journal of Photopolymer Science and Technology 2013;26:555-557.

- [18] Miyamoto K, Ikehara S, Takei H, Akimoto Y, Sakakita H, et al. Red blood cell coagulation induced by low-temperature plasma treatment. Arch Biochem Biophys 2016.
- [19] Binmoeller KF, Thonke F, Soehendra N Endoscopic hemoclip treatment for gastrointestinal bleeding. Endoscopy 1993;25:167-170.
- [20] Zenker M Argon plasma coagulation. GMS Krankenhaushygiene Interdisziplinär 2008;3:Doc15.
- [21] von Woedtke T, Metelmann HR, Weltmann KD Clinical Plasma Medicine: State and Perspectives of in Vivo Application of Cold Atmospheric Plasma. Contributions to Plasma Physics 2014;54:104-117.
- [22] Takamatsu T, Hirai H, Sasaki R, Miyahara H, Okino A Surface Hydrophilization of Polyimide Films Using Atmospheric Damage-Free Multigas Plasma Jet Source. IEEE Transactions on Plasma Science 2013;41:119-125.
- [23] Takamatsu T, Kawano H, Miyahara H, Azuma T, Okino A Atmospheric nonequilibrium mini-plasma jet created by a 3D printer. AIP Advances 2015;5:077184.
- [24] Ryan GE, Pandit AS, Apatsidis DP Porous titanium scaffolds fabricated using a rapid prototyping and powder metallurgy technique. Biomaterials 2008;29:3625-3635.
- [25] Wong KV, Hernandez A A Review of Additive Manufacturing. ISRN Mechanical Engineering 2012;2012:10.
- [26] Iwai T, Albert A, Okumura K, Miyahara H, Okino A, et al. Fundamental properties of a non-destructive atmospheric-pressure plasma jet in argon or helium and its first application as an ambient desorption/ionization source for high-resolution mass spectrometry. Journal of Analytical Atomic Spectrometry 2014;29:464-470.
- [27] Oshita T, Kawano H, Takamatsu T, Miyahara H, Okino A Temperature Controllable Atmospheric Plasma Source. IEEE Transactions on Plasma Science 2015;43:1987-1992.
- [28] Mohamed M, Isfried P, Klaus F, Karl HS Excimer emission from microhollow cathode argon discharges. Journal of Physics D: Applied Physics 2003;36:2922.
- [29] Hofmann S, Gessel AFHv, Verreycken T, Bruggeman P Power dissipation, gas temperatures and electron densities of cold atmospheric pressure helium and argon RF plasma jets. Plasma Sources Science and Technology 2011;20:065010.
- [30] Iwai T, Kakegawa K, Okumura K, Kanamori-Kataoka M, Miyahara H, et al. Fundamental properties of a touchable high-power pulsed microplasma jet and its application as a desorption/ionization source for ambient mass spectrometry. Journal of Mass Spectrometry 2014;49:522-528.
- [31] Chan GCY, Shelley JT, Jackson AU, Wiley JS, Engelhard C, et al. Spectroscopic

plasma diagnostics on a low-temperature plasma probe for ambient mass spectrometry. *Journal of Analytical Atomic Spectrometry* 2011;26:1434-1444.

Figure legends

Fig.1. Overview of the LTP jet

(a) Structure of the 3D printed LTP source; (b) whole LTP source; (c) an image of the endoscope inserted into the LTP source

Fig.2. Experimental setup

(a): Endoscopy of the porcine stomach; (b): Insertion of the biopsy forceps; (c): A bleeding wound made with biopsy forceps; (d): Insertion of the LTP source

Fig. 3. Emissions of various plasmas flowing from the 3D-printed plasma source

Fig. 4. Emission spectra of various gas plasmas, measured using a Maya2000 Pro spectroscope [(200–1100 nm), Ocean Optics, Inc.]

Fig. 5. Endoscopic follow-up of each treated site for five days

(a-1), (b-1), and (c-1): The bleeding wounds made with biopsy forceps before each treatment; (a-2): Immediately after hemostatic clipping; (a-3): One day after hemostatic clipping; (a-4): Three days after hemostatic clipping; (a-5): Five days after hemostatic clipping; (b-2): Immediately after APC-based hemostatic treatment; (b-3): One day after APC-based hemostatic treatment; (b-4): Three days after APC-based hemostatic treatment; (b-5): Five days after APC-based hemostatic treatment; (c-2): Immediately after LTP-based hemostatic treatment; (c-3): One day after LTP-based hemostatic treatment; (c-4): Three days after LTP-based hemostatic treatment; (c-5): Five days after LTP-based hemostatic treatment.

Fig. 6. H&E staining of the normal porcine gastric mucosa

(a): (×4); (a'): (×10)

Fig. 7. H&E staining of the porcine gastric mucosa after each treatment

(a): Clipping-induced hemostasis (×4); (a'): Clipping-induced hemostasis (×10); (b): APC-induced hemostasis (×4); (b'): APC-induced hemostasis (×10); (c): LTP-induced hemostasis (×4); (c'): LTP-induced hemostasis (×10)

Fig. 8. H&E staining of the porcine gastric mucosa at 5 days after each treatment

(a): Clipping-induced hemostasis ($\times 4$); (a'): Clipping-induced hemostasis ($\times 10$); (b): APC-induced hemostasis ($\times 4$); (b'): APC-induced hemostasis ($\times 10$); (c): LTP-induced hemostasis ($\times 4$); (c'): LTP-induced hemostasis ($\times 10$)

Table 1. Parameters of various gas plasmas generated by a 3D printed plasma jet

	Ar	He	O ₂	N ₂	Air	CO ₂
n_e [cm ⁻³]	5.9×10 ¹⁴	2.8×10 ¹⁴	-	-	-	-
P [W]	0.8	0.6	3.1	2.8	1.3	1.8
T_g [°C]	26.9	57.1	37.8	35.0	35.3	41.5

Figure1
[Click here to download high resolution image](#)

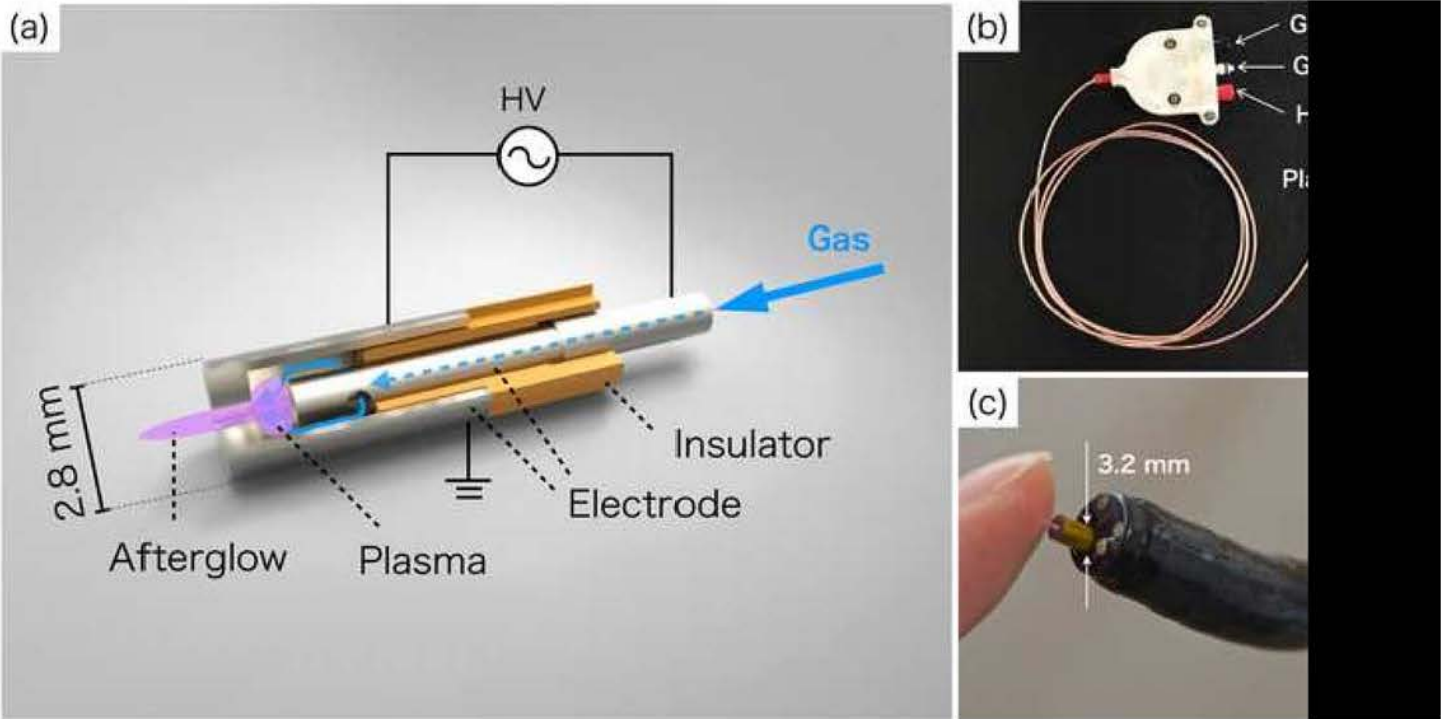


Figure2
[Click here to download high resolution image](#)

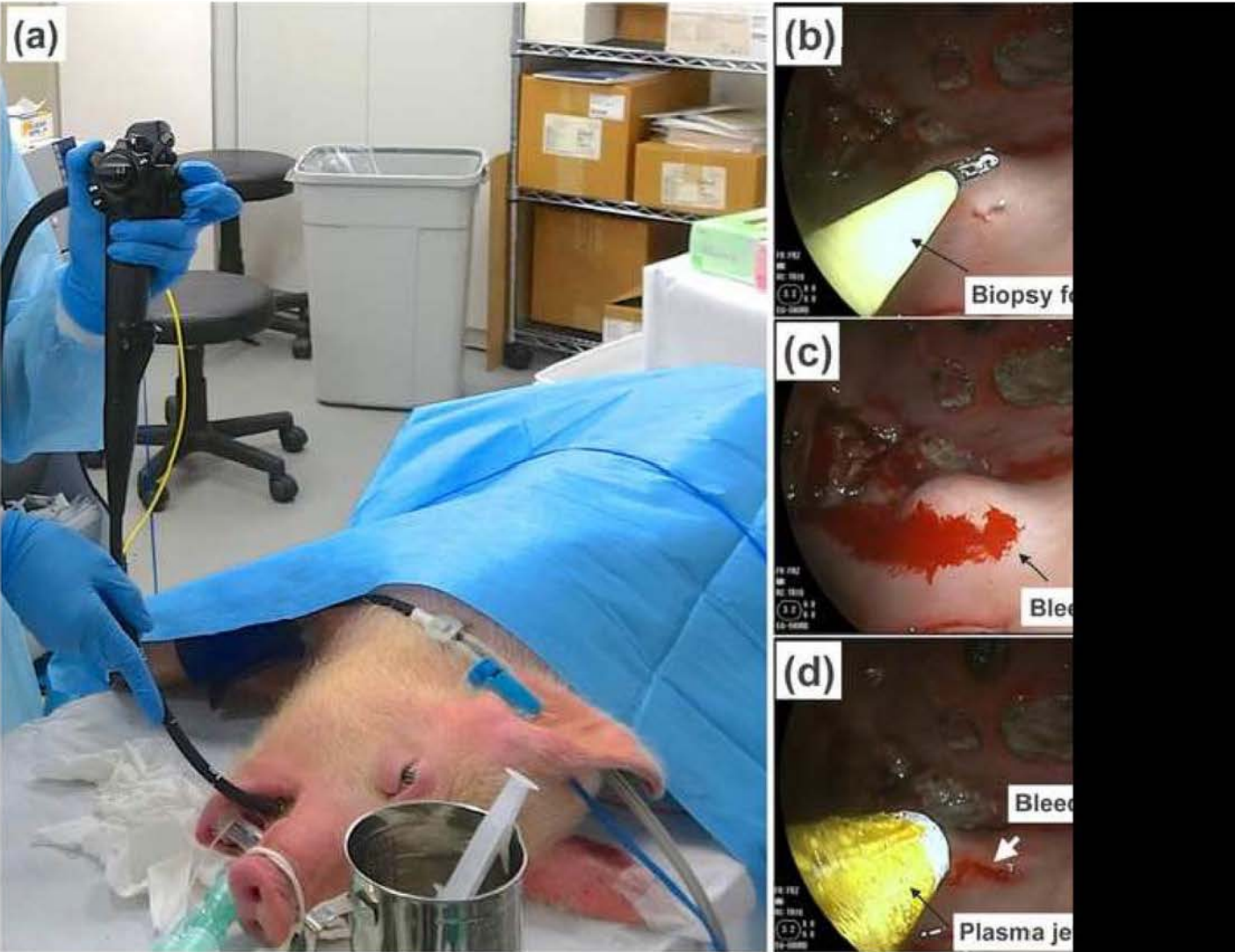


Figure3
[Click here to download high resolution image](#)

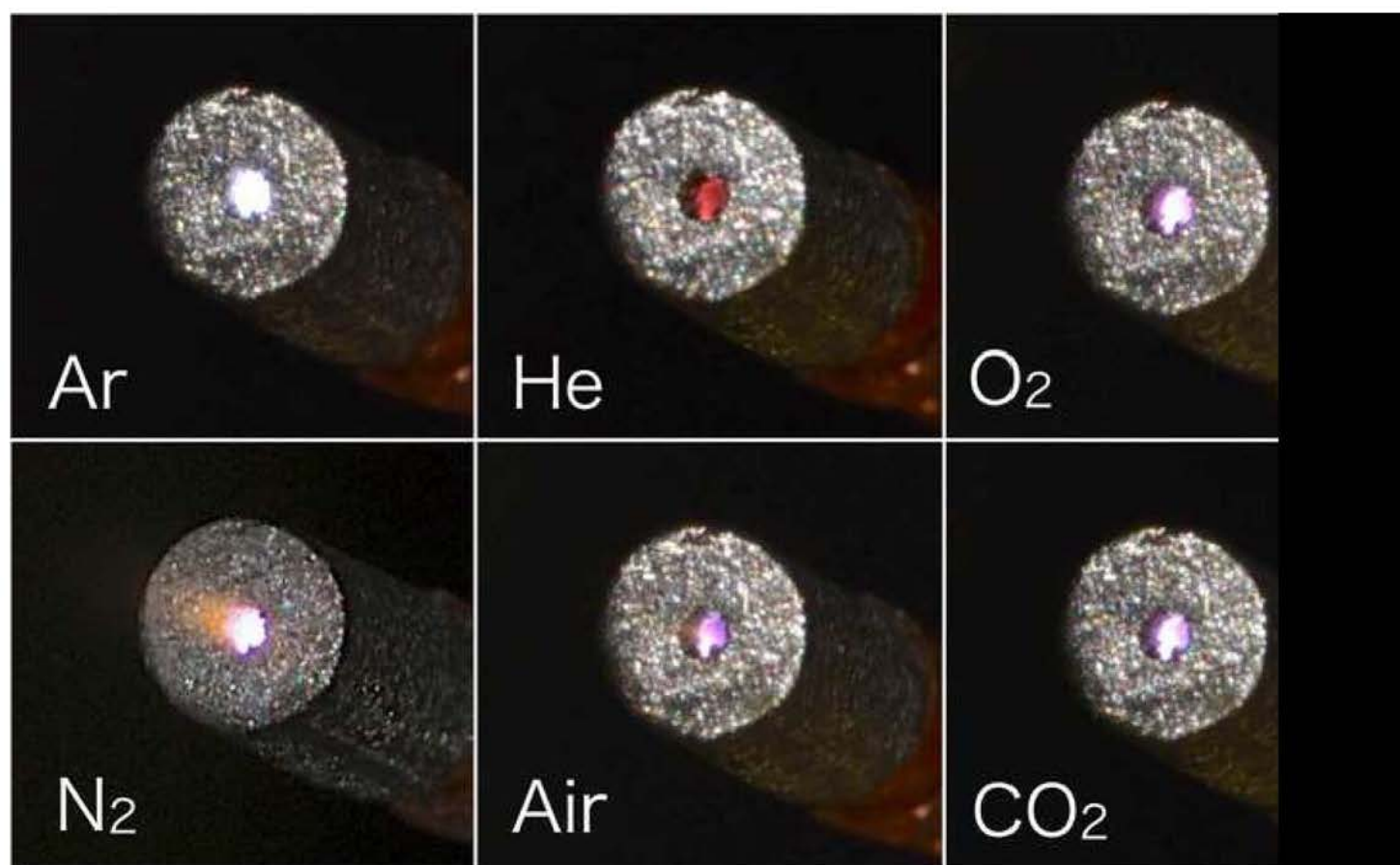


Figure4
[Click here to download high resolution image](#)

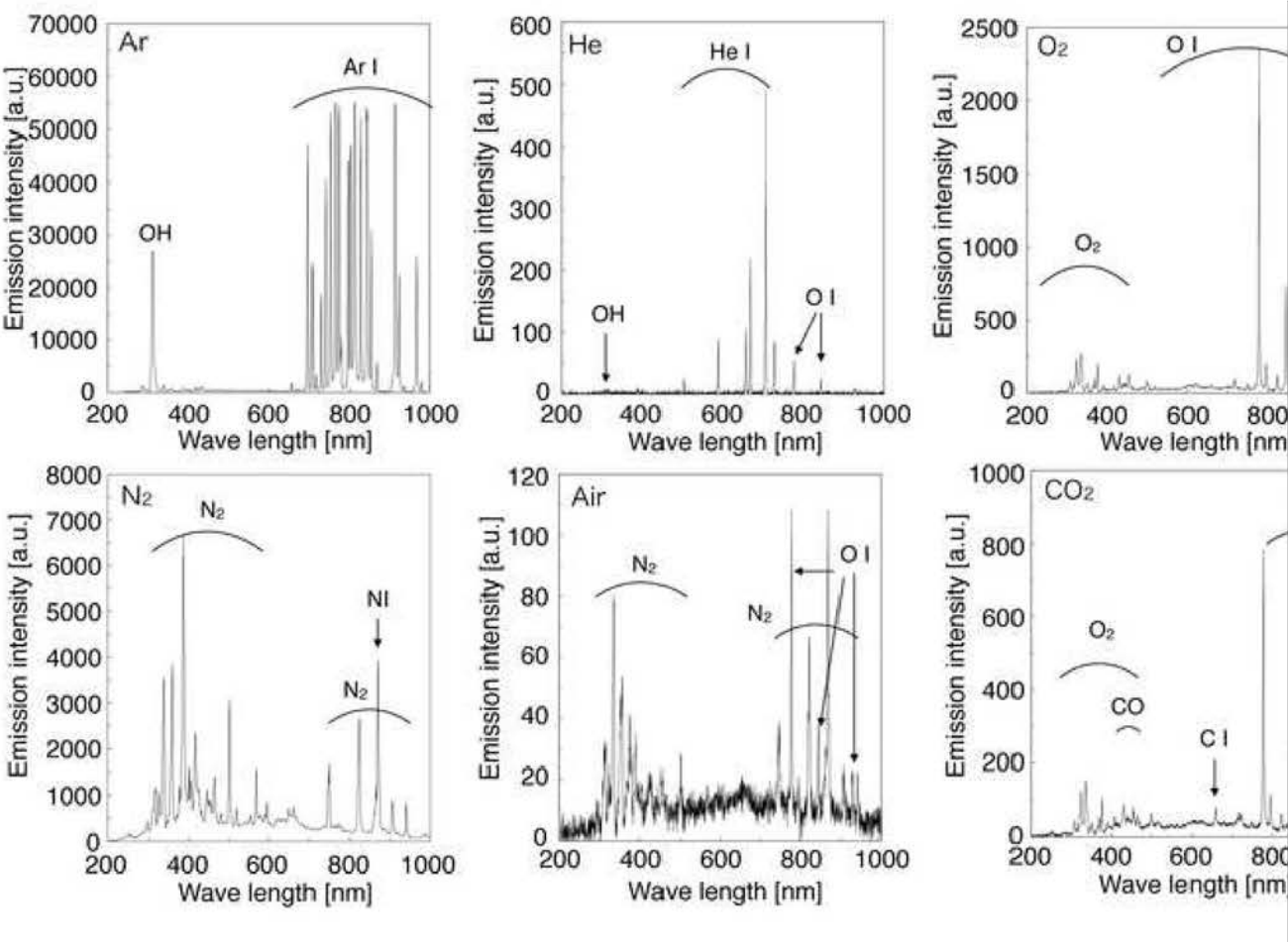


Figure5
[Click here to download high resolution image](#)



Figure6
[Click here to download high resolution image](#)

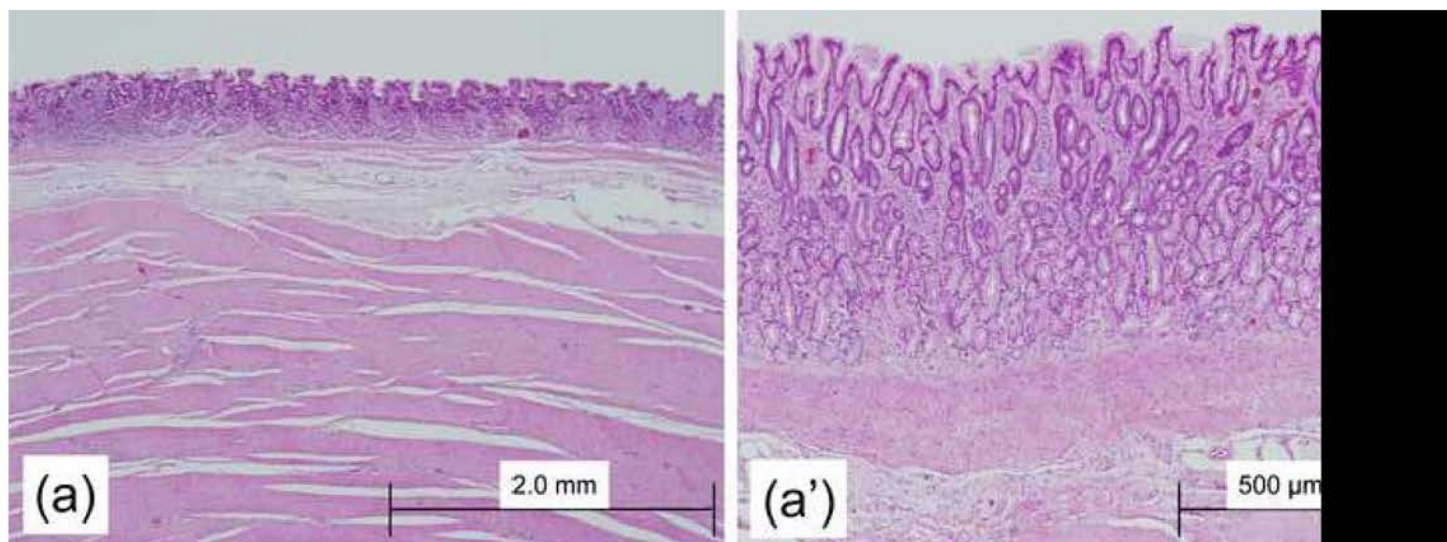


Figure7
[Click here to download high resolution image](#)

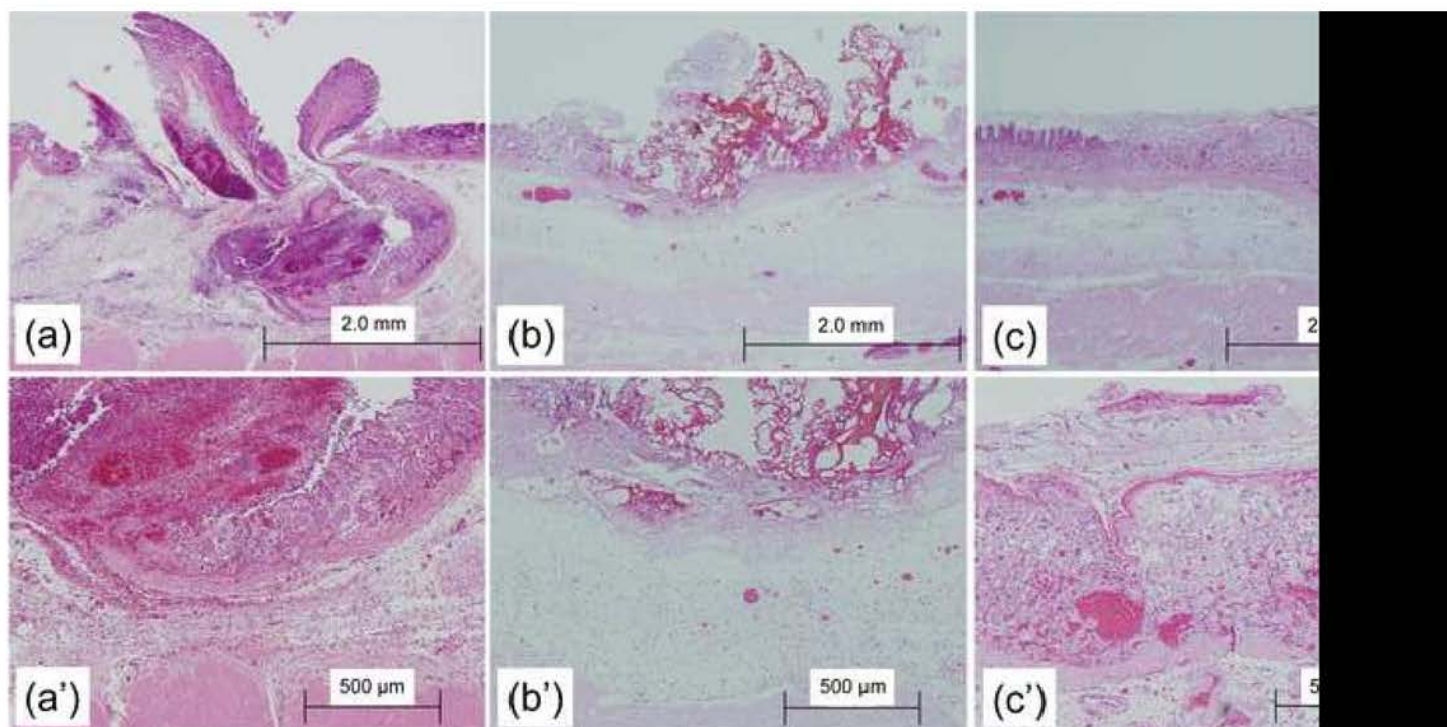


Figure8
[Click here to download high resolution image](#)

